

1 Supporting Information

2 **Efficient Ammonia Photosynthesis from Nitrate by Graphene/Si**

3 **Schottky Junction Integrated with Ni-Fe LDH Catalyst**

4 Chun-Hao Chiang,^{‡a} Yu-Ting Kao,^{‡a} Po-Hsien Wu,^a Ting-Ran Liu,^a Jia-Wei Lin,^b Po-

5 Tuan Chen,^c Jr-Wen Lin,^a Shan-Chiao Yang,^a Hsuen-Li Chen,^a Shivaraj B. Patil,^d Di-

6 Yan Wang ^{*d} and Chun-Wei Chen ^{*abe}

7 ^a Department of Materials Science and Engineering, National Taiwan University,

8 Taipei 10617, Taiwan

9 ^b Center for Condensed Matter Sciences, National Taiwan University, Taipei 10617,

10 Taiwan

11 ^c Department of Vehicle Engineering, National Taipei University of Technology, Taipei

12 10608, Taiwan

13 ^d Department of Chemistry, Tunghai University, Taichung 40704, Taiwan

14 ^e Center of Atomic Initiative for New Materials (AI-MAT), National Taiwan

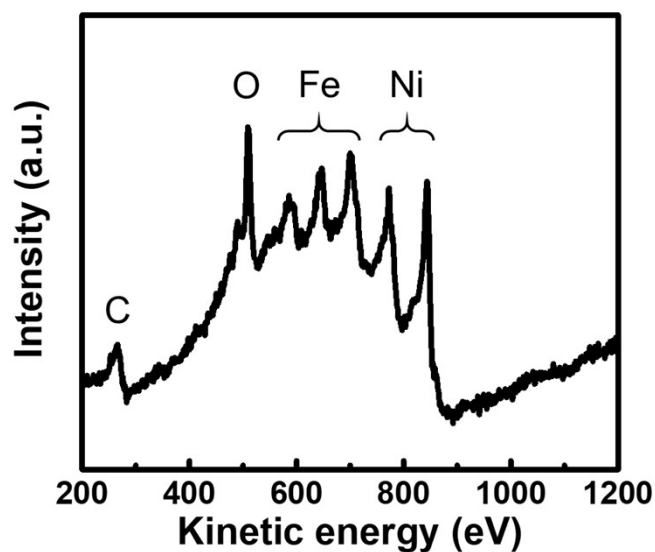
15 University, Taipei 10617, Taiwan

16 [‡] These authors contributed equally to this work.

17 Corresponding author: Di-Yan Wang (E-mail: diyanwang@thu.edu.tw), Chun-Wei

18 Chen (chunwei@ntu.edu.tw)

19

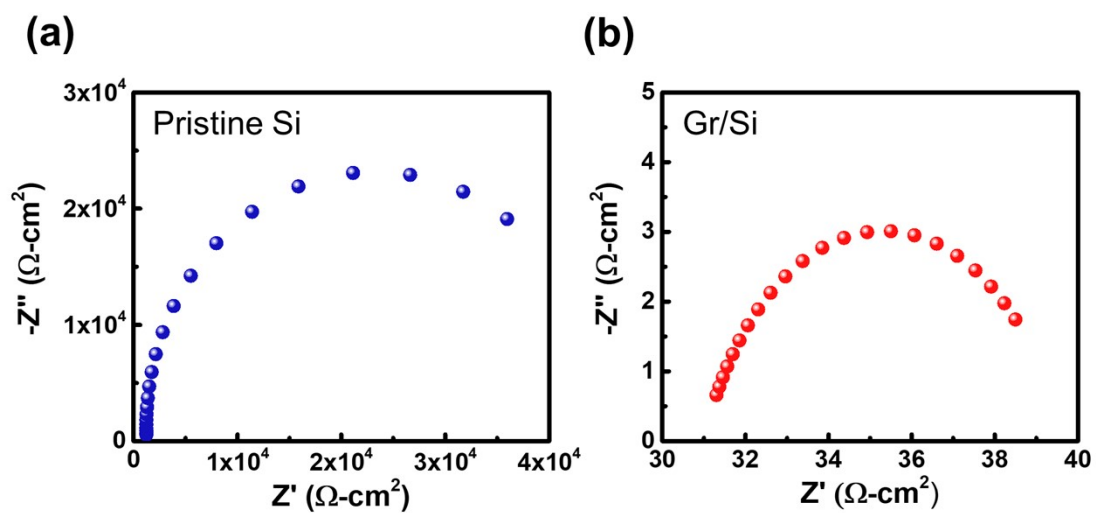


20

21 **Figure S1.** The Auger spectrum of the as-deposited Ni-Fe LDH on graphene/Si
 22 heterojunction.

23

24

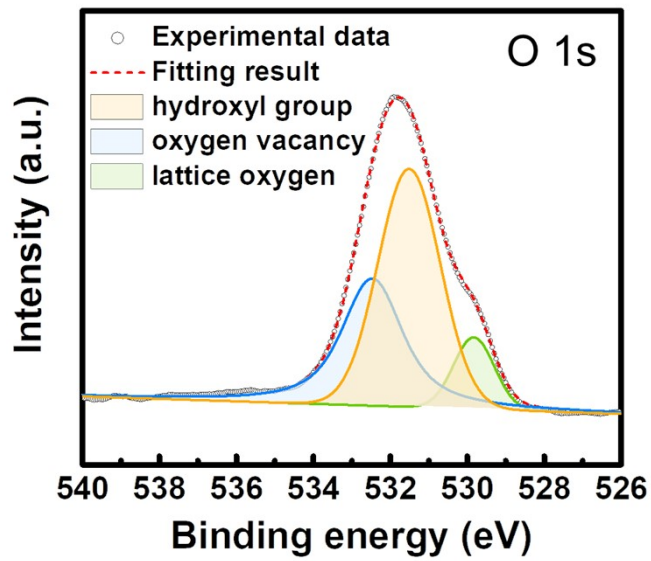


25

26 **Figure S2.** The EIS analysis of the (a) pristine Si and (b) graphene/Si junction in the
 27 electrodeposition solution of Ni-Fe LDH.

28

29

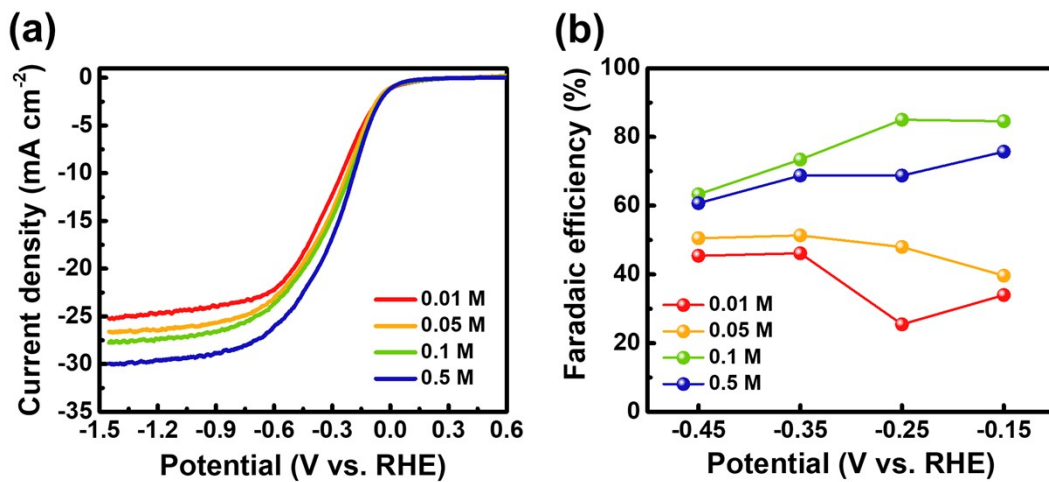


30

31 **Figure S3.** The XPS O 1s spectrum of the as-deposited Ni-Fe LDH.

32

33



34

35 **Figure S4.** The PEC performances of the Ni-Fe LDH/graphene/Si heterojunction

36 photocathode in 0.5 M Na_2SO_4 with various nitrate concentrations (0.01 M, 0.05 M, 0.1

37 M, and 0.5 M). (a) Polarization curves and the (b) corresponding Faradaic efficiencies

38 of the PEC device.

39

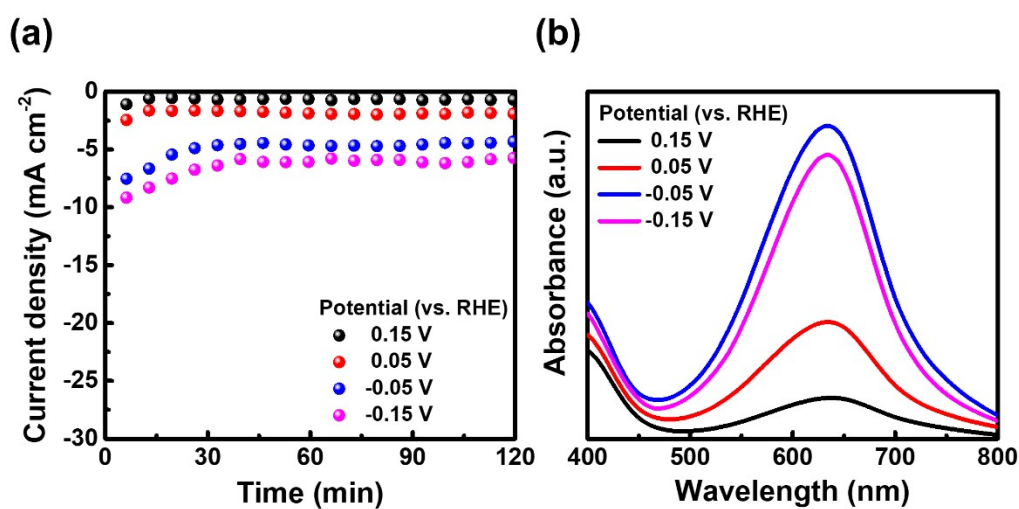
40

Potential (V vs. RHE)	-0.15	-0.25	-0.35	-0.45
FE _{NH₃} (%)	84.57	84.98	74.08	73.01
FE _{NO₂⁻} (%)	3.08	1.78	1.93	2.04

41 **Table S1.** The Faradaic efficiencies of NH₃ and NO₂⁻ products of the Ni-Fe
 42 LDH/graphene/Si PEC cathode under -0.15 V, -0.25 V, -0.35 V, and -0.45 V (vs. RHE)
 43 in 0.5 M Na₂SO₄ and 0.1 M NaNO₃.

44

45

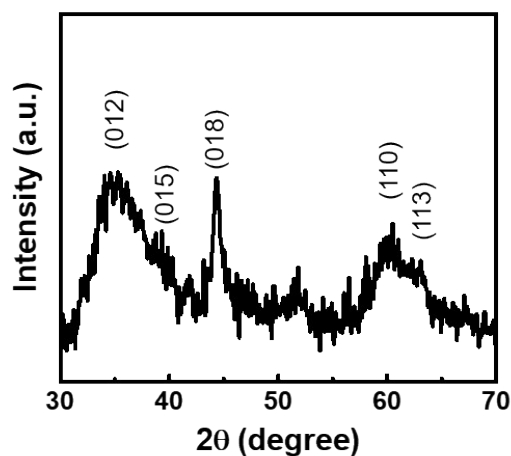


46

47 **Figure S5.** (a) The chronoamperometric curves and (b) absorbance spectra with
 48 indophenol indicator for two-hour measurements of the Ni-Fe LDH/graphene/pyramid
 49 Si heterojunction photocathode.

50

51

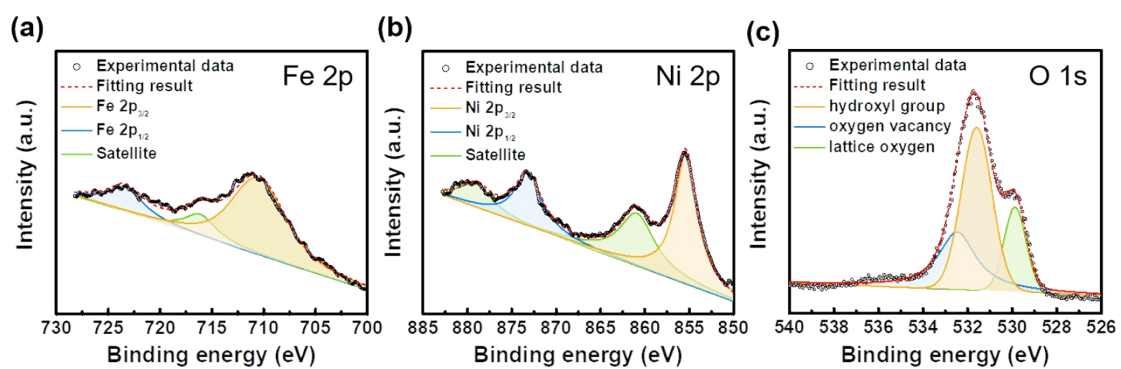


52

53 **Figure S6.** The XRD spectrum of Ni-Fe LDH electrodeposited on pyramid Si.

54

55



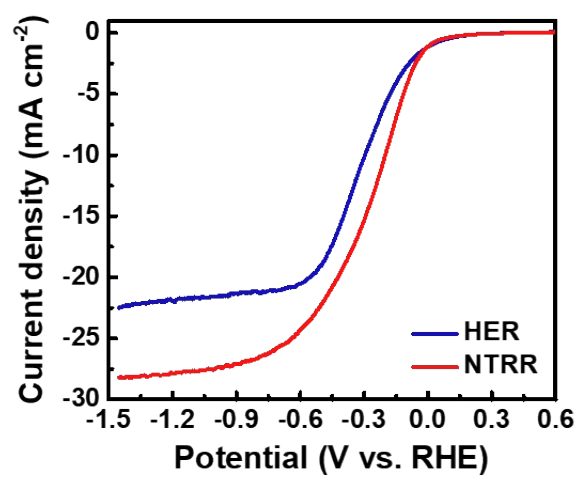
56

57 **Figure S7.** The XPS (a) Fe 2p, (b) Ni 2p, and (c) O 1s spectra of Ni-Fe LDH

58 electrodeposited on pyramid Si.

59

60



61

62 **Figure S8.** The PEC LSV curves of the Ni-Fe LDH/graphene/Si for HER and NTRR.

63 For HER, the electrolyte is 0.5 M Na₂SO₄. For NTRR, the electrolyte is prepared by

64 0.5 M Na₂SO₄ and 0.1 M NaNO₃.

65

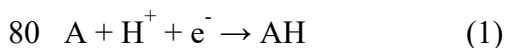
66

67 **DFT calculation:**

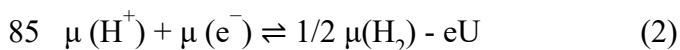
68 The NTRR on Ni-Fe LDH surface model with oxygen vacancy was simulated using
69 Vienna ab initio simulation package (VASP). The model has the vacuum space of larger
70 than 10 Å. The electron-ion interaction was evaluated via the projector augmented-
71 wave (PAW) pseudopotential method, and the exchange-correlation energy functional
72 was covered with the generalized gradient approximation (GGA). The Monkhorst pack
73 k-point grid was set as $2 \times 2 \times 1$ in our calculations for each model. An energy cutoff
74 of 500 eV was used for the plane-wave basis set, and structural relaxation was
75 iteratively performed until the force of each atom was reduced to within 0.01 eV \AA^{-1} .
76 The intermediated states are chosen referred to the literature (ACS Catal. 2019, 9,
77 7052–7064).

78

79 For reactions involving proton and electron transfer,



81 the reaction free energies were estimated through the computational hydrogen electrode
82 model. Specifically, the free energy dependence of the proton–electron pair on the
83 electrode potential was determined using the linear free energy dependence of the
84 electron energy at this potential, which shifts the electron energy by $-eU$,



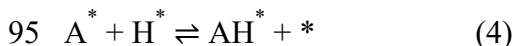
86 where e is the elementary positive charge ($1.602176634 \times 10^{-19} \text{ C}$) and U is the
87 electrode potential on the RHE scale. The free energy change for a specific
88 electrochemical hydrogenation reaction i as a function of potential, $\Delta G_i(U)$, was
89 computed as

$$90 \Delta G_i(U) \rightleftharpoons \Delta E_i + \Delta \text{ZPE} - T\Delta S + eU \quad (3)$$

91 where ΔE_i is the DFT-computed electronic adsorption energy of adsorbate i .

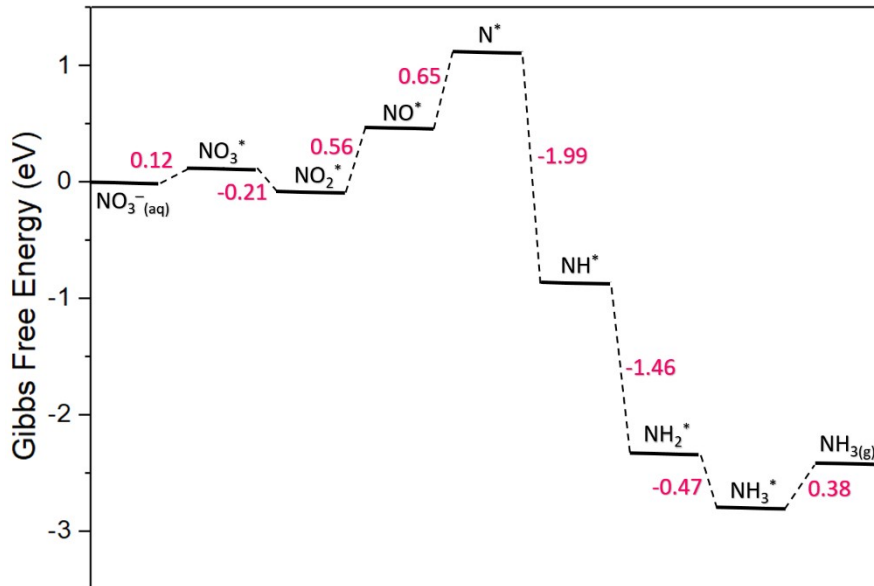
92

93 For computing potential-dependent kinetics, we follow the procedure for
94 nonelectrochemical surface hydrogenation,



96 the activation energy (E_a) can be obtained by DFT calculations of the reactant's
97 minimum-energy geometry and the corresponding hydrogenation transition state. For
98 the corresponding electrochemical step, at equilibrium $\text{H}^+ + \text{e}^- + * \rightleftharpoons \text{H}^*$ conditions, the
99 activation energy $E_a(U^0)$ for $\text{A}^* + \text{H}^+ + \text{e}^- \rightleftharpoons \text{AH}^*$ equals E_a . U^0 is the equilibrium
100 potential at which the analogous nonelectrochemical state, $\mu(\text{H}^*)$, is in equilibrium with
101 its equivalent electrochemical state, $\mu(\text{H}_{(\text{aq})}^+ + \text{e}^-)$. Here, U^0 equals the hydrogen

102 adsorption free energy (ΔG_H) for a given surface at 0 V vs. RHE. The free energy
103 change for the electrochemical surface hydrogenation can then be computed by $U^0 =$
104 $[G(AH^*) - G(A^*) - 1/2G(H_2)]/e$.



105

106 **Figure S9.** The reaction Gibbs free energy diagram of the Ni-Fe LDH with oxygen
107 vacancy on basal plane for nitrate-to-ammonia conversion. The reaction energy barrier
108 of the rate-determining step resulting from NO^* to N^* intermediates is 0.65 eV.